Effect of Elevated Temperatures as a Means of Curing in Inkjet 3D Printed Mortar Specimens

Pshtiwan Shakor[1], Shami Nejadi[2], Gavin Paul[3]
[1]PhD Candidate, Centre for Built Infrastructure Research, University of Technology Sydney
[2]Associate Professor, Centre for Built Infrastructure Research, University of Technology Sydney
[3]Senior Lecturer, Centre for Autonomous Systems, University of Technology Sydney

Abstract: Inkjet (Powder-based) three-dimensional printing (3DP) shows significant promise in concrete construction applications. The accuracy, speed, and capability to build complicated geometries are the most beneficial features of inkjet 3DP. Therefore, inkjet 3DP needs to be carefully studied and evaluated with construction goals in mind and employed in real-world applications, where it is most appropriate. This paper focuses on the important aspect of curing 3DP specimens. It discusses the enhanced mechanical properties of the mortar that are unlocked through a heat-curing process. Experiments have been conducted on cubic mortar samples that have been printed and cured in an oven at a range of different temperatures (e.g. 40, 60, 80, 90, 100°C). The results of the experimental tests have shown that 80°C is the optimum heat-curing temperature to achieve the highest compressive strength and flexural strength of the printed samples. These tests have been performed on two different dimensions of the cubic specimens 20x20x20mm, 50x50x50mm and on prism specimens with the dimensions of 160x40x40mm. The inkjet 3DP process and the post-processing curing are discussed. Additionally, 3D scanning of the printed specimens is employed and the surface roughness profiles of the 3DP specimens are presented.

Graphical Abstract:

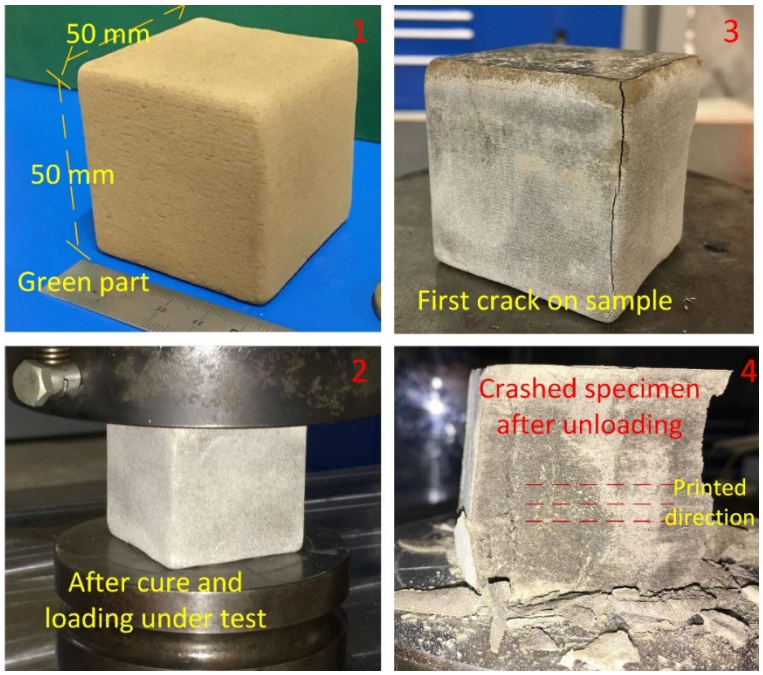

Keywords: Inkjet 3DP, cement mortar, compressive strength, flexural strength, different medium curing, elevated temperature.

1. Introduction

Generally, the most common method in civil engineering is to cast in place or use precast procedures to construct structural members. These structural members are cast using different materials such as concrete, and masonry (Haroglu 2010). Given the ever-increasing need for speed, quality and bespoke design in the construction industry and due to the advances in rapid prototyping, the procedures for constructing structural members should be reconsidered and upgraded (Shakor, Nejadi, Paul & Malek 2019).

According to the earlier studies, three main methods for the 3DP powder-bed process have been recognized (Lowke et al. 2018) as follows: i) selective binder (cement) activation, ii) binder jetting and iii)

selective paste intrusion, respectively (Shakor, Renneberg, et al. 2017) (Paul et al. 2018) (Shakor, Nejadi & Paul 2019). The selective binder (cement) activation is the process that is used in this paper, which is usually known as powder-bed printing (binder/inkjet printing) (Shakor, Sanjayan, et al. 2017) (Shakor et al. 2018) (Shakor, Nejadi, Paul, Sanjayan, et al. 2019).

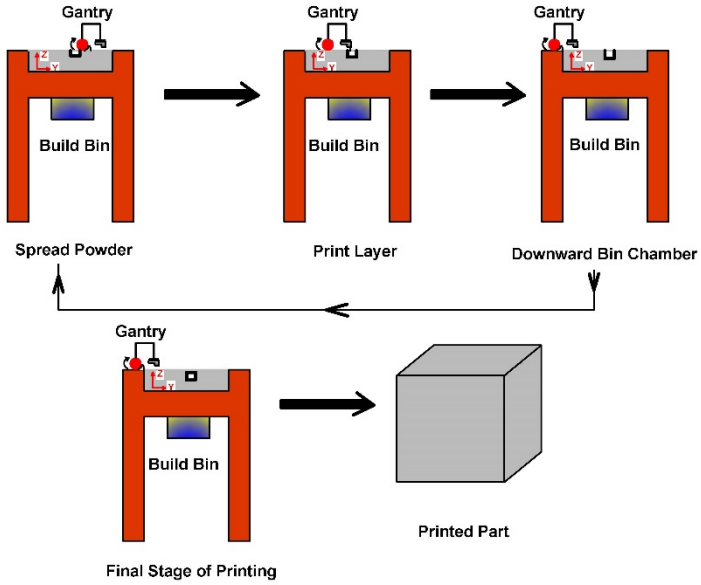

Figure 1. Schematic depiction of the powder-bed printing (layer technique) in inkjet 3D printing.

Figure 1 shows how inkjet 3DP can be used as a multi-layer process to complete a structure using powder-based materials and an activator such as water.

Concretes commonly provide enough fire resistance for most normal applications. Nevertheless, the strength of concrete declines at elevated temperatures due to chemical and physical deviations (Kodur 2014). At high temperatures, the spalling of conventional concrete happens which result in a rapid layer-by-layer loss of concrete surface, and most significantly can expose the reinforcement bars in the concrete to fire (Sanjayan & Stocks 1993). This has motivated significant research efforts to the application of different types of cement at different temperatures so as to find the optimum strength and optimum heat resistance for concrete. Concurrent research is also being conducted into the use of fibre reinforcement to enable concrete and mortar to exhibit improved mechanical properties (Li & Maalej 1996).

The objective of this study is to experimentally scrutinise the performances of 3DP mortar in the inkjet printing technique under elevated temperatures. This investigation also studied the effects of sample size on the printed mortar. To evaluate the mechanical strength of the 3DP mortar at a variety of different temperatures, the bending and compressive strength tests executed for the printed mortar.

2. Materials and methodology

2.1 Materials

The modified mix that has been used for inkjet 3DP in this research, contains 67.8% of Calcium Aluminate Cement (CAC) ranging sieve (75- 150μm), 32.2% of Ordinary Portland Cement (OPC) and 5% of fine sand as a percentage of total weight. Figure 2 displays the curve of the cumulative distribution of the custom-made powder (cement mortar powder) (CP) and ZP 151 original materials in terms of the particle size. ZP 151 contains (80-90%) of calcium sulphate hemihydrate ($CaSO_4 \cdot 0.5H_2O$) which is produced by the 3DSystems (3DSystems 2013).

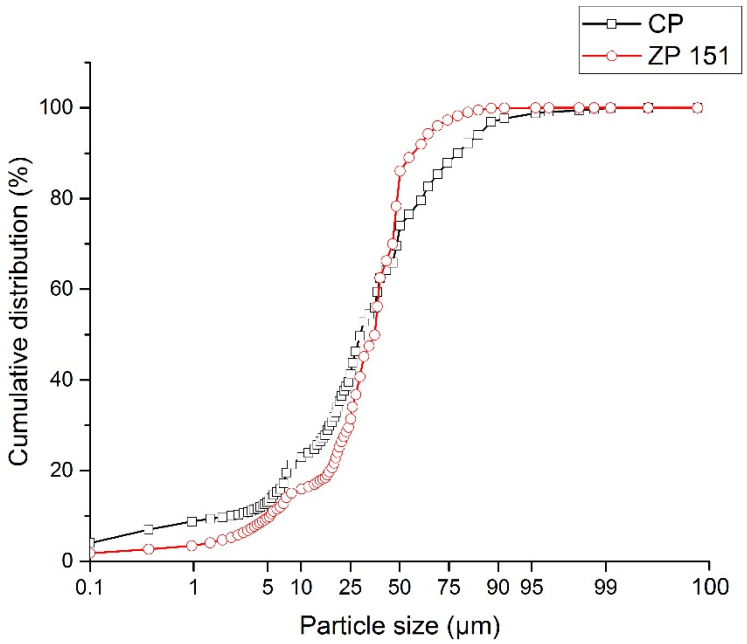

Figure 2. The curve of particle size distributions of the original ZP 151 and custom-made (CP) powder.

Figure 3 shows the modified mix proportion powder (cement mortar CP), that replaces the original powder ZP 151. The modified powder has been mixed properly by employing a Hobart mixer at a speed of 1450 revolutions per minute.

Furthermore, the homogeneity and consistency of the powder are vital factors that must be controlled when in pursuit of superior resolutions and results. Hence, the speed of the mixer and therefore the time of blending has been shown to be the main contributor to the homogeneity of the powder and production of higher quality 3DP objects (Hill, Orr & Dunne 2008).

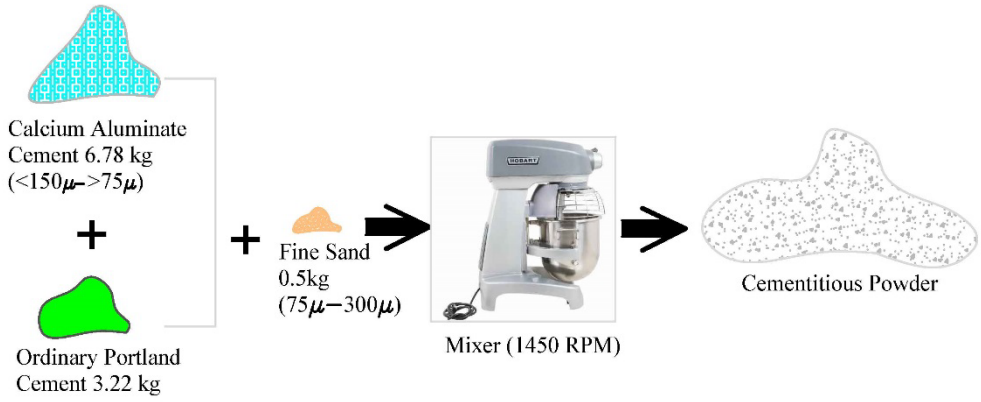

Figure 3. Schematic illustration of the process for preparing cementitious powder.

2.2 Methodology

Samples with dimensions of 20×20×20mm and 50×50×50mm have been prepared for a compressive strength test. In addition, prism samples with dimensions of 160×40×40mm have been prepared for a flexural strength test. As shown in Table (1), three samples have been prepared for each test. Figure 4 shows the green part (without any post-processing) for a 3DP mortar as a prism (a), and as a cube (b). The green part is the name given to completion fabricated part after printing and removal from the build-chamber, but prior to commencing any post-processing procedures (Shakor, Sanjayan, et al. 2017).

Table 1. Detailed number and dimension of samples

Sample description	CAD dimensions	Number of samples	Printed direction plane
Cube	(20×20×20)	54	XY, XZ, YZ
Cube	(50×50×50)	54	XY, XZ, YZ
Prism	(160×40×40)	18	XZ

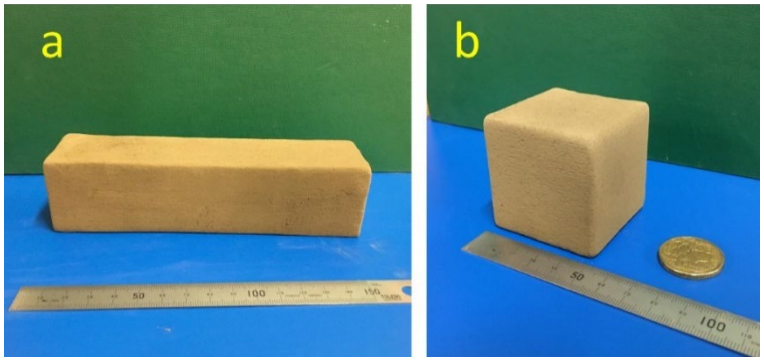

Figure 4. (a) Green part of 3DP cement mortar prism, (b) green part of 3DP cement mortar cube.

3. Results and discussions

Figure 5 shows the results of the compressive strength of printed mortar samples. The presented results belong to the specimens that have been cured in tap water only, (3-hour 40°C, 28-day water, 3-hour 40°C), (3-hour 60°C, 28-day water, 3-hour 60°C), etc. However, after a sample is printed, the proper post-processing consists of (a) curing in the oven for 3-hours; (b) curing for 28-days in tap water then; (c) drying in the oven for 3-hours. These basic post-processing sequences (a, b & c) are used for all samples but with various temperatures until the optimized maximum compressive strength of the printed sample is found.

Figure 5 shows the compressive strength test outcomes for the sets of printed specimens that have been properly cured for 28-days at five different temperatures. The graph bars with indicated values on top are the actual strengths and error bars indicate the standard deviations of the result. As shown in Figure 5, an increase in the curing temperature from 40 to 80 °C leads to a near-linear increase in compressive strength. This increased strength in the cement mortar which is proportional to the increase in temperatures could be due to the greater reaction level of cement mortar at elevated temperatures. Curing in an oven accelerates the reaction of the cementitious process. Fast hydration and a high early compressive strength have been observed to occur as the temperature increases (Lothenbach et al. 2007).

The experimental results are consistent with the study conducted by Abd elaty (2014) which demonstrated that the compressive strength of Portland cement concrete with a low w/c ratio at 50°C is higher than at lower temperatures (e.g. 10°C and 23°C). Early mechanical strength development for compressive strength and a trend of increased strength have been repeatedly observed even at 91 days for cement mortar at temperatures of 60°C (Amin et al. 2017).

Raised temperature increases the rate of reaction and reduces the setting time (Shakor et al. 2018) since it accelerates the dissolving of alumina and silica particles from the un-reaction particles of the powder and a larger amount of Alumina (Al_2O_3) and Silica(SiO_2) becomes available for the reaction process. The modified powder for 3DP contains a high proportion of Alumina due to the high levels of CAC in the main powder. In relation to the total mass, Al_2O_3 contributes approximately 70% in CAC, whereas it is only 5% in general purpose cement.

Binder has a significant effect on the result of compressive strength at high temperatures due to the main content of the binder that has isopropyl alcohol. Binder consists of humectant and water, where humectant is 2-pyrrolidone (3DSystems 2012).

Despite the trend observed up to 80°C, a contrary trend was observed when the temperature rose beyond 80°C up to 90°C, as shown in Figure 5. According to previous studies (Altan & Erdoğan 2012), a threshold temperature for the cementitious reaction process will occur when temperature-controlled kinetics is inhibited. Extra Al_2O_3 and SiO_2 particles are reacted while the curing temperature is above the threshold

point. Mortar slurry forms rapidly and is deposited on the surface of the unreacted powder, which will constrain further dissolution. Consequently, the compressive strength declines significantly. Hence, 80°C was nominated as the optimum curing temperature for cement mortar samples.

In general, curing in tap water achieves low compressive strength test results, predominantly due to the slight reaction that occurs among particles. The small concentration of OH- ions in tap water works as a reactive chemical agent in the cementitious process since it leads to ineffective dissolution and formation of hydroxyl substances (Bellego, Gérard & Pijaudier-Cabot 2000) (Sagoe-Crentsil & Weng 2007). Consequently, low compressive strength will emerge due to the densify reaction not being established appropriately. Additionally, it must be noted that water curing at high temperatures adversely affect the compressive strength, due to heat acceleration which leads to the leaching of Al_2O_3 and SiO_2 from the existing gel in the samples.

Samples for the compressive test were printed and tested in all three planes. This study has shown that the compressive strength is predictably influenced by the printed plane direction of the sample. The YZ printed plane exhibited noticeably lower compressive strength results, while for the XY and XZ planes the results are generally similar for the 20mm cubes (Figure 5a) and XY was overwhelmingly better in the 50mm cubes (Figure 5b).

These results are positive for the construction industry and precast construction applications. This study utilised optimal saturation levels that were presented in the authors' earlier studies (Shakor, Sanjayan, et al. 2017), (Shakor et al. 2018), (Shakor, Nejadi, Paul, Sanjayan, et al. 2019) to show the strongest plane and direction along with the optimised elevated temperature, which is most suitable for medium curing to gain the highest compressive strength.

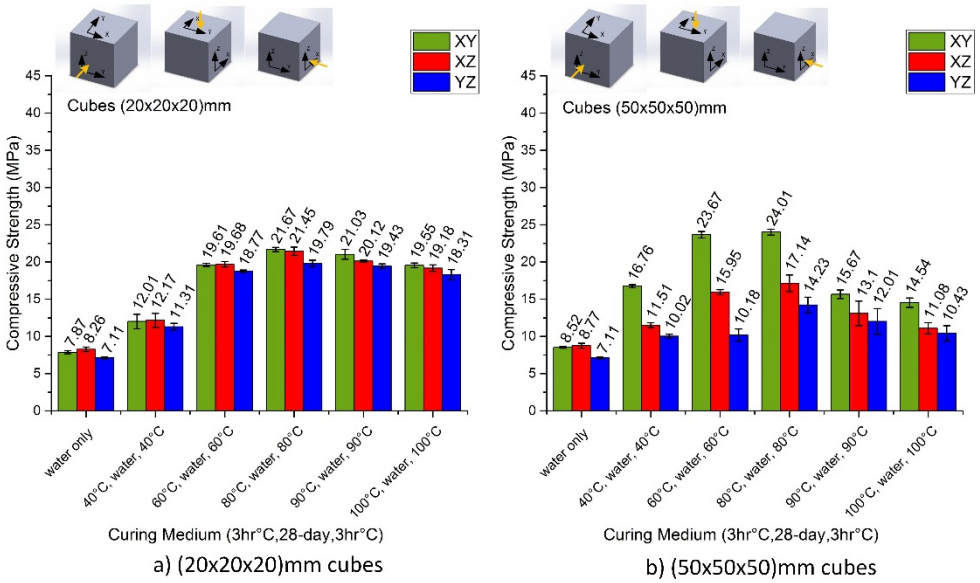

Figure 5. Compressive strength of mortar sample using different curing medium for (a) 20×20×20mm cubes and (b) 50×50×50mm

The prism specimens have been prepared and conducted for the three-point bending test (ASTMC293/C293M 2002). The size of the samples has been chosen based on the conventional standard prism for the mortar.

As shown in Figure 6, investigation on the mechanical properties by three-point bending test reveals higher flexural strengths at the temperature degree (80°C). Clearly, the 80°C curing temperature has a better performance than other cured temperature. It has been observed in Figure 7 that the printed specimens which cured at 90°C and 100°C has cracks on the surface due to elevated temperature and evaporated water content.

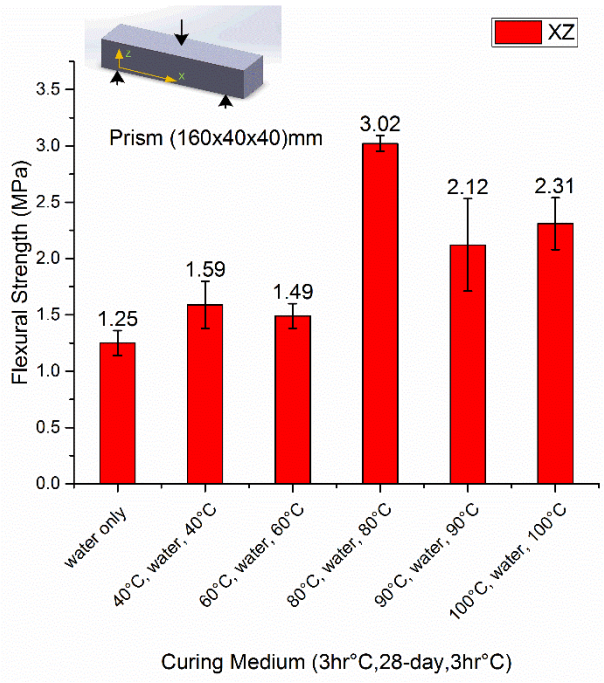

Figure 6. Flexural strength of mortar sample 160×40×40mm using different temperature medium.

Abdulkareem et al. (2014) explained that the compressive strength for mortar and geopolymer declines when the elevated temperature is very high (i.e. 400°C, 600°C, 800°C). It was also found that the mortar and geopolymer paste experience the higher strength loss as the temperature increases, where the best result is in the 70°C (Abdulkareem et al. 2014). This agrees with the results from the presented study for the cement mortar-based 3DP objects that have been tested under various temperatures conditions.

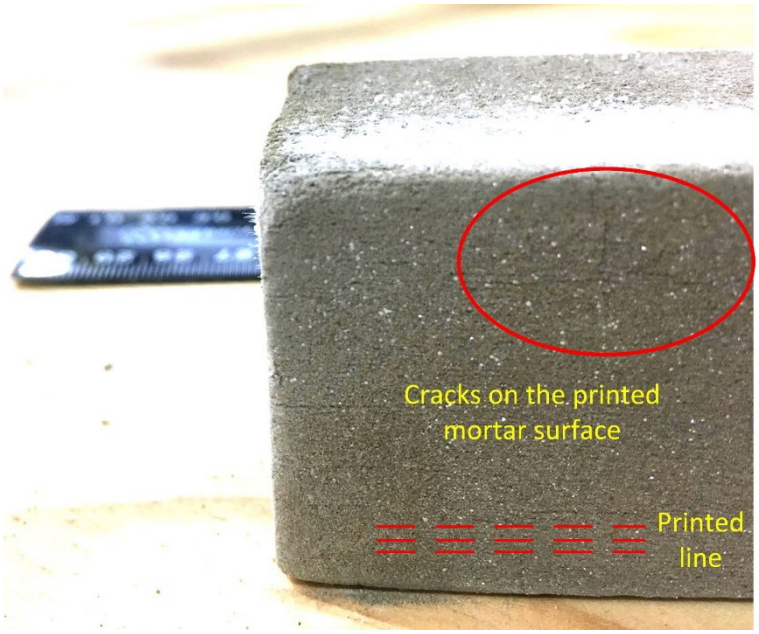

Figure 7. Prism mortar sample 160×40×40mm after removed from the oven at 90°C temperature.

The results displayed in Figure 5 demonstrate that the size influences the printed specimens; contrary to conventional casted specimens, where increasing the size printed specimens increases the mechanical strength. This phenomenon could be due to a better flowability from the feeder tank and better compaction on the build-chamber for the bigger samples. The feeder tank contains a rotor motor which is in the middle of the printer. Therefore, the powders for the bigger samples deposit from the middle of the feeder tank with more homogeneity and lesser voids between particles. This results in a better deposition of powder and

more powder flowing from the feeder. When the powders have more particles in the feeder chamber, the result is that the roller spreads more powder on the build-chamber and the powder in the build-chamber is more effectively getting compacted.

Figure 8 shows the roughness profile and the images of the surface morphology of the printed specimens at different magnifications (20x, 50x, 100x). Obvious holes and valleys are shown on the printed specimens. The blurring in the images occurs where there are different heights on the surface. The average surface roughness on the surface of the cement mortar is 22.31±3.72μm, which is slightly higher than the recommended powder's (gypsum) result of 13.76±0.95μm. This means the cement powder's surface is rougher than the gypsum and has more valleys on the surface of printed objects.

The roughness on the surface mortar varies from position to position due to the inconsistency of distributing cement mortar powders in the build-chamber. It has been observed that the powder particle distribution for the recommended materials (gypsum) in the build-chamber are evenly distributed which results in a higher resolution and smooth surface on the printed sample.

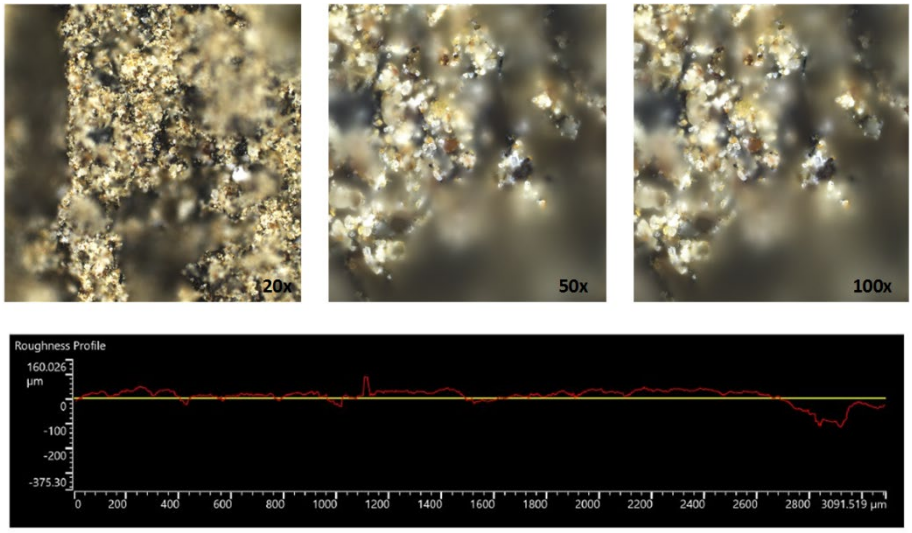

Figure 8. Surface roughness profile and images captured of the surface of printed cement mortar in 20×, 50×, and 100×, the bottom image showed the roughness profile compared with the mean line.

4. Conclusions

In conclusion, 3DP technology is emerging as an advanced technique to construct highly precise and complicated structures, which are conventionally difficult to fabricate. This study has investigated the elevated temperature effects on the printed mortar samples. Compressive strength tests have been conducted on the sets of different sized cubic samples and flexural strength tests have been performed on one set of rectangular prism samples. Results have revealed that the larger size samples have higher mechanical strength. Furthermore, the maximum compressive strength and flexural strength can be achieved when a post-processing curing procedure at an elevated temperature of 80°C has been utilized. Further works on inkjet 3DP need to be investigated, specifically on the post-processing medium, and infiltration. Ideally, the future work can be focused on broader applications for construction purposes, such as an investigation on larger-scale prints in real-life.

5. Acknowledgements

The authors acknowledge the support of UTS's ProtoSpace and the Civil Engineering laboratory.

6. References

1. 3DSystems 2012, 'ZB63 Safety Data Sheet', Series ZB63 Safety Data Sheet.
2. 3DSystems 2013, 'ZP151 Powder Safety Data Sheet', Series ZP151 Powder Safety Data Sheet.
3. Abd elaty, M.a.a. 2014, 'Compressive strength prediction of Portland cement concrete with age using a new model', *HBRC Journal*, vol. 10, no. 2, pp. 145-55.

4. Abdulkareem, O.A., Mustafa Al Bakri, A.M., Kamarudin, H., Khairul Nizar, I. & Saif, A.e.A. 2014, 'Effects of elevated temperatures on the thermal behavior and mechanical performance of fly ash geopolymer paste, mortar and lightweight concrete', *Construction and Building Materials*, vol. 50, pp. 377-87.
5. Altan, E. & Erdoğan, S.T. 2012, 'Alkali activation of a slag at ambient and elevated temperatures', *Cement and Concrete Composites*, vol. 34, no. 2, pp. 131-9.
6. Amin, M.N., Khan, K., Saleem, M.U., Khurram, N. & Niazi, M.U.K. 2017, 'Aging and curing temperature effects on compressive strength of mortar containing lime stone quarry dust and industrial granite sludge', *Materials*, vol. 10, no. 6, p. 642.
7. ASTMC293/C293M 2002, '293 Standard Test Method for Flexural Strength of Concrete (Using Simple Beam With Center-Point Loading)', *ASTM Standard*.
8. Bellego, C.L., Gérard, B. & Pijaudier-Cabot, G. 2000, 'Chemo-mechanical effects in mortar beams subjected to water hydrolysis', *Journal of Engineering Mechanics*, vol. 126, no. 3, pp. 266-72.
9. Haroglu, H. 2010, 'Investigating the structural frame decision making process', © Hasan Haroglu.
10. Hill, J., Orr, J. & Dunne, N. 2008, 'In vitro study investigating the mechanical properties of acrylic bone cement containing calcium carbonate nanoparticles', *Journal of Materials Science: Materials in Medicine*, vol. 19, no. 11, pp. 3327-33.
11. Kodur, V. 2014, 'Properties of concrete at elevated temperatures', *ISRN Civil engineering*, vol. 2014.
12. Li, V.C. & Maalej, M. 1996, 'Toughening in cement based composites. Part II: Fiber reinforced cementitious composites', *Cement and Concrete Composites*, vol. 18, no. 4, pp. 239-49.
13. Lothenbach, B., Winnefeld, F., Alder, C., Wieland, E. & Lunk, P. 2007, 'Effect of temperature on the pore solution, microstructure and hydration products of Portland cement pastes', *Cement and Concrete Research*, vol. 37, no. 4, pp. 483-91.
14. Lowke, D., Dini, E., Perrot, A., Weger, D., Gehlen, C. & Dillenburger, B. 2018, 'Particle-bed 3D printing in concrete construction – Possibilities and challenges', *Cement and Concrete Research*.
15. Paul, S.C., van Zijl, G.P., Tan, M.J. & Gibson, I. 2018, 'A review of 3D concrete printing systems and materials properties: Current status and future research prospects', *Rapid Prototyping Journal*, no. just-accepted, pp. 00-.
16. Sagoe-Crentsil, K. & Weng, L. 2007, 'Dissolution processes, hydrolysis and condensation reactions during geopolymer synthesis: Part II. High Si/Al ratio systems', *Journal of Materials Science*, vol. 42, no. 9, pp. 3007-14.
17. Sanjayan, G. & Stocks, L. 1993, 'Spalling of high-strength silica fume concrete in fire', *Materials Journal*, vol. 90, no. 2, pp. 170-3.
18. Shakor, P., Nejadi, S. & Paul, G. 2019, 'A Study into the Effect of Different Nozzles Shapes and Fibre-Reinforcement in 3D Printed Mortar', *Materials*, vol. 12, no. 10, p. 1708.
19. Shakor, P., Nejadi, S., Paul, G. & Malek, S. 2019, 'Review of Emerging Additive Manufacturing Technologies in 3D Printing of Cementitious Materials in the Construction Industry', *Frontiers in Built Environment*, vol. 4, no. 85.
20. Shakor, P., Nejadi, S., Paul, G. & Sanjayan, J. 2018, 'A Novel Methodology of Powder-based Cementitious Materials in 3D Inkjet Printing for Construction Applications ', paper presented to the *Sixth International Conference on the Durability of Concrete Structures*, Leeds, UK.
21. Shakor, P., Nejadi, S., Paul, G., Sanjayan, J. & Nazari, A. 2019, 'Mechanical Properties of Cement-Based Materials and Effect of Elevated Temperature on Three-Dimensional (3-D) Printed Mortar Specimens in Inkjet 3-D Printing', *Materials Journal*, vol. 116, no. 2, pp. 55-67.
22. Shakor, P., Renneberg, J., Nejadi, S. & Paul, G. 2017, 'Optimisation of Different Concrete Mix Designs for 3D Printing by Utilising 6DOF Industrial Robot', paper presented to the *ISARC. Proceedings of the International Symposium on Automation and Robotics in Construction*, Taipei, Taiwan.
23. Shakor, P., Sanjayan, J., Nazari, A. & Nejadi, S. 2017, 'Modified 3D printed powder to cement-based material and mechanical properties of cement scaffold used in 3D printing', *Construction and Building Materials*, vol. 138, pp. 398-409.